Aalborg Universitet

AALBORG UNIVERSITY
DENMARK

On Uncertainty Investigation of mmWave Phased Array Element Control with an All-on Method

Gao, Huaqiang; Fan, Wei; Wang, Weiming; Zhang, Fengchun; Wang, Zhengpeng; Wu, Yongle ; Liu, Yuanan; Pedersen, Gert Frølund

On Uncertainty Investigation of mmWave Phased Array Element Control with an All-on Method

Huaqiang Gao, Wei Fan, Weimin Wang, Fengchun Zhang, Zhengpeng Wang, Yongle Wu, Yuanan Liu, and Gert Frølund Pedersen

Abstract—Accurate control of complex excitation of array elements is key to ensure spatial discrimination capability of millimeter-wave (mmWave) phased array, e.g. beamforming to target signal directions and nulling towards interference signal directions. Element excitation uncertainties are typically evaluated in an "on-off" mode, where the element under test is enabled with other phased array elements properly terminated. However, such an "on-off" method might lead to inaccurate results due to the fact that mmWave phased arrays are typically designed for an "all-on" mode, where all array elements are enabled with proper complex excitations. Therefore, there is a need to accurately determine the array element excitation uncertainties in its typical operation mode, i.e. "all-on" mode. In this letter, an "all-on" method is proposed to enable accurate array element uncertainty investigation in the "all-on" mode. The proposed algorithm is experimentally validated in a 4×4 mmWave phased-array experimental platform. The experimental results have shown that an amplitude deviation up to ±0.1 dB and a phase deviation ±1° can be achieved in the "all-on" mode with the proposed method, compared to those up to ±0.8 dB and ±9°, respectively for the conventional "on-off" method.

Index Terms—Millimeter-wave (mmWave) antenna-in-package (AiP), phased array calibration, antenna measurement, uncertainty analysis.

I. Introduction

MILLIMETER-WAVE (mmWave) phased arrays have been widely adopted to provide high gain and multi-stream transmission with electronically steerable beamforming for mmWave mobile communications [1], [2]. As a mainstream antenna and packaging solution for mmWave applications, antenna-in-package (AiP) technology integrates mmWave antennas in chip packages and has been widely employed in mmWave radio and radar systems [3]. With the AiP design, the mmWave phased array is capable of controlling the element excitations in beamformer radio frequency integrated circuits (RFICs) to achieve the reconfigurable radiation pattern. For example, by adjusting the phase weights of elements,

Huaqiang Gao, Weimin Wang, Yongle Wu, and Yuanan Liu are with the Beijing Key Laboratory of Work Safety Intelligent Monitoring, Department of Electronic Engineering, Beijing University of Posts and Telecommunications, Beijing 100876, China (e-mail: gaohq@ieee.org; wangwm@bupt.edu.cn; wuyongle138@gmail.com; and yuliu@bupt.edu.cn).

Wei Fan, Fengchun Zhang, and Gert Frølund Pedersen are with the Antenna Propagation and Millimeter-wave Systems (APMS) section, Department of Electronic Systems, Faculty of Engineering and Science, Aalborg University, Aalborg 9220, Denmark (e-mail: gfp@es.aau.dk).

Zhengpeng Wang is with the Electronics and Information Engineering, Beihang University, Beijing 100191, China (e-mail: wangzp@buaa.edu.cn).

main beam and nulls can be steered to the target and interfering signal directions, respectively. Sidelobes can be suppressed by applying tapered amplitude weights. Besides, a plane wave can be approximated over a finite volume in a given region by allocating complex weights to the array elements [4].

The performance of mmWave phased array is deeply dependent on the accurate control of array element. However, the element control has errors in practice. The control accuracy could bring important influence on the phase array performance. Moreover, there exists the large chip-to-chip variation in amplitude and phase response at mmWave AiP. The bad control accuracy of mmWave AiP will become the bottle-neck for the mmWave applications with accurate phase and amplitude control requirement. Therefore, the uncertainty analysis and evaluation of phased array element is of significant importance to ensure the phased array performance.

In the conventional method, the control uncertainty is typically evaluated in an "on-off" mode, i.e. to enable one element sequentially each time. A probe antenna is placed in the far field to record element excitation variation. However, the measurement accuracy suffers from link budget issues due to the large measurement distance, especially at mmWave frequency bands. Another way is to place a probe antenna in a near field scanner where the probe antenna is moved to the front of antenna element with equal distance, which is typically adopted in the industry. However, the precise mechanical positioning is laborious and expensive due to some practical factors, e.g. the "black box" design of AiP and the surface fluctuation of the planar near-field scanner. The uncertainty analysis in the "on-off" mode requires that the isolation between antenna elements are high enough [5]. However, this is typically not the case for mmWave phased array AiP because the mutual coupling effect is non-negligible in mmWave AiPs with current AiP design [6], [7]. Since the normal working mode of the mmWave phased array AiP is an "all-on" mode in practical applications (e.g. beamforming and nulling), the uncertainty analysis performed in the "on-off" mode might be inaccurate or even misleading. Therefore, it would be more reasonable and accurate to evaluate the element control uncertainty of mmWave AiP in the "all-on" mode, i.e. all elements of AiP are enabled. This is, however, largely overlooked in the literature.

This letter proposes a novel "all-on" method to enable the uncertainty analysis of mmWave phased array in the "all-on" mode. The element control uncertainty is investigated by the deviation between the practical excitation increment and the desired setting increment. Referring to the array

Fig. 1. Measurement configuration for mmWave phased array AiP element uncertainty analysis.

Fig. 2. Illustration of excitation acquisition principle in phasor notation.

calibration, the practical excitation increment is detected in the "all-on" mode for single element. The proposed method is experimentally validated and its effectiveness is demonstrated in contrast with the conventional "on-off" method.

II. THEORY

A. AiP element complex excitation acquisition

To avoid the large measurement error of phase at mmWave frequencies, the rotating-element electric-field vector (REV) calibration method [8]–[10] based on power-only measurement is preferred for the AiP element complex excitation acquisition in this letter. For the purposes of uncertainty investigation in an "all-on" mode of this letter, the primary principle of REV method needs to be revisited in the following. Fig. 1 shows the measurement setup for the complex excitation acquisition of AiP elements in an "all-on" mode. Under certain initial phase shifts of N elements, the original composite complex field $\dot{E}_0$ of an AiP with N elements is a superposition of the electric field of N elements, expressed in phasor notation as

$$\dot{E}_0 = \sum_{n=1}^{N} \dot{E}_n = \sum_{n=1}^{N} \dot{h}_n \dot{x}_n = \boldsymbol{H}\boldsymbol{x} = A_0 e^{j\Phi_0}, \quad (1)$$

where $\dot{E}_n$ is the complex field of the nth element. $\boldsymbol{x} = \{\dot{x}_n\} \in \mathbb{C}^{N \times 1}$ with its nth element $\dot{x}_n = A_n e^{j\Phi_n}$ is the complex excitation vector for N AiP elements. $\boldsymbol{H} = \{\dot{h}_n\} \in \mathbb{C}^{1 \times N}$ is a transfer matrix between N AiP element feeds and the probe antenna feed, with its nth element $\dot{h}_n = \alpha_n e^{j\varphi_n}$.

During the excitation acquisition of the nth element, as illustrated in Fig. 2, the phase excitation of the nth element is tuned by Δ, whereas the other $N-1$ elements remain unchanged. The updated composite field $\dot{E}_0'$ is expressed as a function of the phase tuning Δ of the nth element, i.e.

$$\dot{E}_0'(\Delta) = \dot{E}_0 - \dot{E}_n + \dot{E}_n e^{j\Delta}$$
$$= A_0 \left[e^{-j(\Phi_n + \varphi_n - \Phi_0)} + \frac{\alpha_n A_n}{A_0}(e^{j\Delta} - 1) \right] \quad (2)$$
$$\cdot e^{j(\Phi_n + \varphi_n)}.$$

The relative amplitude k_n and phase X_n of the electric field $\dot{E}_n$ of the nth element with respect to the original composite field $\dot{E}_0$ is defined as

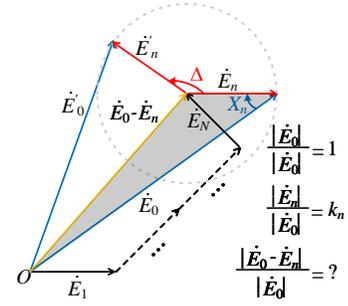$$k_n = \frac{|\dot{E}_n|}{|\dot{E}_0|} = \frac{\alpha_n A_n}{A_0}, \quad (3)$$

$$X_n = \Phi_n + \varphi_n - \Phi_0. \quad (4)$$

Substituting (3) and (4) into (2), we have

$$\dot{E}_0'(\Delta) = A_0 \big[(\cos X_n + k_n \cos \Delta - k_n) $$
$$+ j(k_n \sin \Delta - \sin X_n) \big] \cdot e^{j(X_n + \Phi_0)} \quad (5)$$
$$= A_0' e^{j\Phi_0'}.$$

The power $A_0'^2$ of the updated composite field $\dot{E}_0'$ is

$$A_0'^2(\Delta) = A_0^2 \cdot$$
$$\left[Y_n^2 + k_n^2 + 2Y_n k_n \left(\frac{\cos X_n - k_n}{Y_n} \cos \Delta - \frac{\sin X_n}{Y_n} \sin \Delta \right) \right]$$
$$= A_0^2 \left[(Y_n^2 + k_n^2) + 2Y_n k_n \cos(\Delta + \Delta_0) \right], \quad (6)$$

where we have

$$Y_n = \sqrt{(\cos X_n - k_n)^2 + \sin^2 X_n}, \quad (7)$$

$$\tan \Delta_0 = \frac{\sin X_n}{\cos X_n - k_n}. \quad (8)$$

On the basis of (6) with Δ tuned from $0°$ to $360°$ (i.e. one turn), we obtain

$$r = \frac{A_0'\big|_{\max}}{A_0'\big|_{\min}} = \frac{Y_n + k_n}{|Y_n - k_n|}, \quad (9)$$

The solutions for k_n and X_n are obtained by solving the equations of (7), (8), and (9) together. According to the inequality relations of Y_n and k_n, we have two sets of solutions for k_n and X_n in [8]. The solutions are just determined by the ratio r in (9), and the phase Δ_0 achieving $A_0'^2\big|_{\max}$ in (6).

From (7), we have

$$Y_n^2 = 1 + k_n^2 - 2k_n \cos X_n. \quad (10)$$

Combining (10) and Fig. 2 applying the Law of Cosines, we obtain $Y_n = |\dot{E}_0 - \dot{E}_n|/|\dot{E}_0|$, where $|\dot{E}_0 - \dot{E}_n|$ stands for the composite field amplitude of all elements except the nth element. Since $|\dot{E}_0 - \dot{E}_n| > |\dot{E}_n|$ is held for practical phased arrays in general, the solutions for k_n and X_n under $Y_n > k_n$ are adopted. Therefore, in thes "all-on" mode, the excitation amplitude A_n and phase Φ_n of the nth element under certain initial phase shift are acquired by $k_n A_0/\alpha_n$ and $X_n + \Phi_0 - \varphi_n$, respectively. M complex excitations of the nth element under M settings of initial phase shift are acquired for the element uncertainty analysis in the following.

B. AiP element control uncertainty analysis

The element control uncertainty is measured by the deviation between the practical excitation increment and the desired setting increment. For the sake of simplicity, the focus of this letter is on the control accuracy of phase shifter. From Section II-A, we acquire the complex excitation $\dot{x}_{n,m} = A_{n,m}e^{j\Phi_{n,m}}$ of the nth element under the mth setting of initial phase shift $\phi_{n,m}$. The initial phase shift is set from $0°$ to $360°$ with a uniform step of ψ, i.e. the mth setting of initial phase shift $\phi_{n,m} = (m-1)\psi$.

The excitation increment of the nth element under the setting of initial phase shift $\phi_{n,m}$ versus the setting of $0°$ is

$$\frac{\dot{x}_{n,m}}{\dot{x}_{n,1}} = \frac{A_{n,m}e^{j\Phi_{n,m}}}{A_{n,1}e^{j\Phi_{n,1}}} = \frac{A_{n,m}}{A_{n,1}}e^{j(\Phi_{n,m}-\Phi_{n,1})}, \quad (11)$$

where

$$\frac{A_{n,m}}{A_{n,1}} = \frac{k_{n,m}A_{0,m}}{\alpha_n} \bigg/ \frac{k_{n,1}A_{0,1}}{\alpha_n} = \frac{k_{n,m}A_{0,m}}{k_{n,1}A_{0,1}}, \quad (12)$$

$$\Phi_{n,m} - \Phi_{n,1} = (X_{n,m} - X_{n,1}) + (\Phi_{0,m} - \Phi_{0,1}). \quad (13)$$

In (13), $\Phi_{0,m}$ and $\Phi_{0,1}$ are the phase of the original composite field $\dot{E}_{0,m}$ and $\dot{E}_{0,1}$ under the setting of initial phase shift $\phi_{n,m}$ and $0°$ for the nth element, respectively. In the classical REV calibration [8], the relative excitations among elements are obtained under the common original composite field. In this letter, the relative excitations of single element are obtained under different settings of initial phase shift. Therefore, the original composite field is not constant. The phase variation of original composite field is largely overlooked in the literature. Because of the power-only measurement during the excitation acquisition in Section II-A, the phase measurement of the original composite field is not available. For this reason, the term of $\Phi_{0,m} - \Phi_{0,1}$ in (13) is calculated synthetically in the following to compensate the phase variation of the original composite field.

The original composite field $\dot{E}_{0,m}$ and updated composite field $\dot{E}'_{0,1}$ under the setting of initial phase shift $\phi_{n,m}$ and $0°$ for the nth element respectively are

$$\dot{E}_{0,m} = \dot{E}_{0,1} - \dot{E}_{n,1} + \dot{E}_{n,1}e^{j\phi_{n,m}}, \quad (14)$$

$$\dot{E}'_{0,1}(\Delta) = \dot{E}_{0,1} - \dot{E}_{n,1} + \dot{E}_{n,1}e^{j\Delta}. \quad (15)$$

Combining (14) and (15), we have $\dot{E}_{0,m} = \dot{E}'_{0,1}(\phi_{n,m})$, i.e. $\Phi_{0,m} = \Phi'_{0,1}(\phi_{n,m})$. From (5), the phase $\Phi'_{0,1}$ of the updated composite field $\dot{E}'_{0,1}$ under the setting of initial phase shift $0°$ is expressed as

$$\Phi'_{0,1}(\Delta) = \tan^{-1}\frac{k_{n,1}\sin\Delta - \sin X_{n,1}}{\cos X_{n,1} + k_{n,1}\cos\Delta - k_{n,1}} + X_{n,1} + \Phi_{0,1}. \quad (16)$$

According to the results of complex excitation acquisition under the setting of initial phase shift $0°$ in Section II-A (i.e. $k_{n,1}$ and $X_{n,1}$ are known), the phase variation of the original
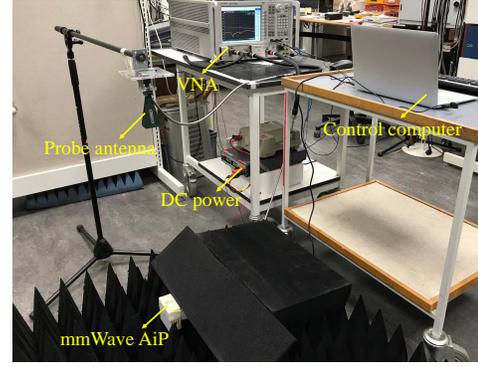

Fig. 3. Photograph of measurement setup.

composite field under the setting of initial phase shift $\phi_{n,m}$ relative to the setting of $0°$ is calculated by

$$\begin{aligned}&\Phi_{0,m} - \Phi_{0,1}\\&= \Phi'_{0,1}(\phi_{n,m}) - \Phi'_{0,1}(\phi_{n,1})\\&= \tan^{-1}\frac{k_{n,1}\sin((m-1)\psi) - \sin X_{n,1}}{\cos X_{n,1} + k_{n,1}\cos((m-1)\psi) - k_{n,1}} + X_{n,1}.\end{aligned} \quad (17)$$

III. MEASUREMENT VALIDATION

In this section, the proposed "all-on" algorithm is experimentally validated in a phased array experimental platform developed at Aalborg University. The measurement setup is demonstrated in Fig. 3. The mmWave AiP contains a 4×4 array of 16 patch elements with half wavelength spacing at 28 GHz. The AiP element complex excitation can be arbitrarily set by the control computer. In our measurement, all elements of AiP are set to be active and the phase shift of only one element is set in each control. The attenuation setting of the element is kept the same (e.g. 0 dB). The complex scattering parameter S between mmWave AiP feed and probe antenna feed is measured by a vector network analyzer (VNA) at 28 GHz for the excitation acquisition and uncertainty investigation of AiP element. The relative change (amplitude or phase) of the scattering transmission parameter S is equivalent to that of the composite field of AiP elements. Based on the relative change, the element excitation can be acquired and the element control uncertainty can be investigated from Section II. Note that our proposed method is based on the amplitude-only measurement. The phase of S measurement is utilized just to validate our phase compensation technique, as discussed later. Taking the first element of AiP for example where $n=1$ and $\psi = 5.625°$ (i.e. $M = 65$), the measured amplitude results with 65×65 S measurements are shown in Fig. 4.

The uncertainty investigation in both "on-off" and "all-on" modes is to set the initial phase shift that is linearly progressing from $0°$ to $360°$ with a step of $5.625°$ and to measure the field variation. The complex and amplitude-only measurements are required in the "on-off" and "all-on" modes, respectively. Since only one element is enabled in the "on-off" mode, the element excitation increment under different settings of initial phase shift can be detected directly from
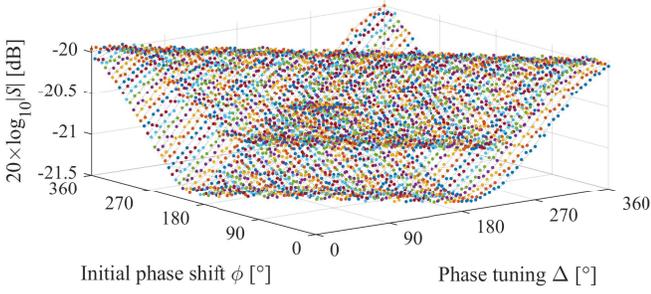
Fig. 4. Measured amplitude of the scattering transmission parameter S with 65×65 measurements in the "all-on" mode.
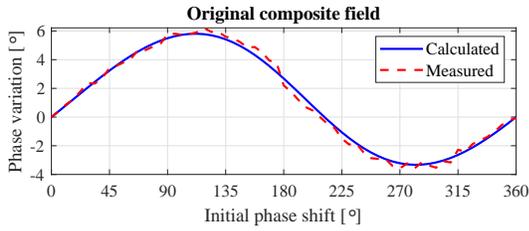

Fig. 5. Phase variation of the original composite field under different settings of initial phase shift.

Fig. 6. Phase uncertainty results before and after the phase compensation.

Fig. 7. Comparison of control uncertainty between the proposed "all-on" method and the conventional "on-off" method.

the measured complex field variation. This method, however, cannot achieve the detection for the uncertainty investigation of one element with other elements enabled or coupled. In the "all-on" mode, specifically, under each setting of initial phase shift, an extra phase tuning technique in Section II-A is employed to acquire the element excitation, with a uniform tuning step of $5.625°$ (i.e. a total of 65×65 measurements for all settings of initial phase shift, as shown in Fig. 4). The error between the excitation phase increment and the setting increment of initial phase shift is evaluated for the uncertainty investigation in the following. Note that during the excitation acquisition of element, the measured $|S|^2$ under each setting of initial phase shift is fitted best by a cosinusoidal curve to acquire more accurate excitation results, as indicated in (6).

To verify the feasibility of the phase compensation in Section II-B, the phase change information of the composite field is extracted from the measured S. Fig. 5 depicts the phase variation of the original composite field under different settings of initial phase shift. The synthetic phase variation calculated in (17) matches well with the measured one, which validates the effectiveness of phase compensation. It is required for the phase compensation technique to only utilize the results of complex excitation acquisition under the setting of initial phase shift $0°$, independent of the array configuration. In contrast with the phase uncertainty result without the phase compensation, the compensated one is shown in Fig. 6. The phase uncertainty is $±5°$ and $±1°$ before and after the phase compensation, respectively. Obviously, smaller phase uncertainty is observed after the phase compensation. With the proposed phase compensation technique, the deviation introduced by the unknown phase variation of composite field can be compensated well to evaluate more accurate phase uncertainty.
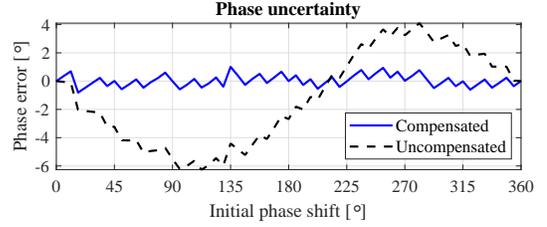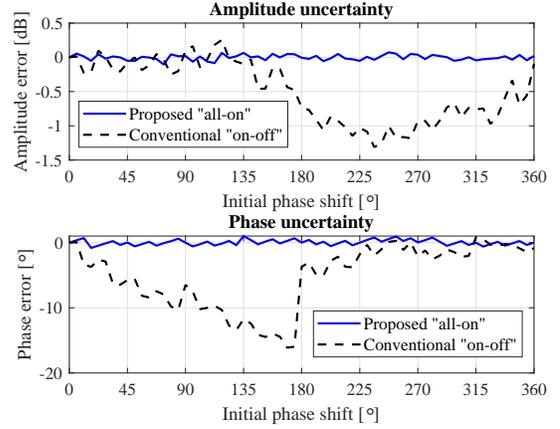
Finally, the evaluation results of control uncertainty are compared between the proposed "all-on" method and the conventional "on-off" method in Fig. 7. In the conventional "on-off" method, the amplitude and phase uncertainty are $±0.8$ dB and $±9°$ for the first element, respectively. For other elements, the maximum amplitude and phase uncertainty can be up to $±2.5$ dB and $±13°$, respectively. In the proposed "all-on" method of this letter, the amplitude and phase uncertainty are $±0.1$ dB and $±1°$, respectively. The uncertainty results in the "on-off" mode might be misleading and inaccurate, while they are more accurate and more realistic in the "all-on" mode. Although the focus of this letter is on the phase uncertainty of the element control (via setting the element attenuation to 0 dB in each control), the proposed "all-on" method can be well applied for both amplitude and phase uncertainty investigation of the AiP element control.

IV. CONCLUSION

In this letter, an "all-on" method for evaluating element control uncertainty of mmWave phased array AiP is proposed and validated in an "all-on" mode. The proposed method validates the control uncertainty of single element in the "all-on" mode of AiP, where a phase compensation technique needs to be introduced. In the "all-on" mode, each element can be controlled well within a small uncertainty (i.e. amplitude $±0.1$ dB and phase $±1°$), while large control uncertainty is seen (i.e. amplitude $±0.8$ dB and phase $±9°$) in the conventional "on-off" mode. The evaluation results of control uncertainty in the "all-on" mode of AiP have more instruction and reference value in practical applications, instead of the "on-off" mode.

REFERENCES

[1] W. Hong, K.-H. Baek, and S. Ko, "Millimeter-Wave 5G Antennas for Smartphones: Overview and Experimental Demonstration," *IEEE Transactions on Antennas and Propagation*, vol. 65, no. 12, pp. 6250–6261, Dec. 2017.

[2] A. Valdes-Garcia, B. Sadhu, X. Gu, J.-O. Plouchart, M. Yeck, and D. Friedman, "Scaling Millimeter-Wave Phased Arrays: Challenges and Solutions," *2018 IEEE BiCMOS and Compound Semiconductor Integrated Circuits and Technology Symposium (BCICTS)*, Oct. 2018.

[3] Y. Zhang and J. Mao, "An Overview of the Development of Antenna-in-Package Technology for Highly Integrated Wireless Devices," *Proceedings of the IEEE*, vol. 107, no. 11, pp. 2265–2280, Nov. 2019.

[4] F. Scattone, D. Sekuljica, A. Giacomini, F. Saccardi, A. Scannavini, L. J. Foged, E. Kaverine, N. Gross, and P. O Iversen, "Comparative Testing of Devices in a Spherical Near Field System and Plane Wave Generator," *2019 Antenna Measurement Techniques Association Symposium (AMTA)*, pp. 1–3, Oct. 2019.

[5] F. Zhang, W. Fan, Z. Wang, Y. Zhang and G. F. Pedersen, "Improved Over-the-Air Phased Array Calibration Based on Measured Complex Array Signals," *IEEE Antennas and Wireless Propagation Letters*, vol. 18, no. 6, pp. 1174–1178, June 2019.

[6] X. Chen, M. Abdullah, S. Zhang, T. Li, and Q. Li, "Mutual Coupling Reduction of Slot Array Antenna for 5G Millimeter-wave Handset," *2019 Photonics and Electromagnetics Research Symposium – Fall (PIERS – Fall)*, pp. 1525–1530, Dec. 2019.

[7] X. Chen, M. Abdullah, Q. Li, J. Li, A. Zhang, and T. Svensson, "Characterizations of Mutual Coupling Effects on Switch-Based Phased Array Antennas for 5G Millimeter-Wave Mobile Communications," *IEEE Access*, vol. 7, pp. 31376–31384, March 2019.

[8] S. Mano and T. Katagi, "A method for measuring amplitude and phase of each radiating element of a phased array antenna," *Trans. IECE*, vol. J65-B, no. 5, pp. 555–560, May 1982.

[9] T. Takahashi, Y. Konishi, and I. Chiba, "A Novel Amplitude-Only Measurement Method to Determine Element Fields in Phased Arrays," *IEEE Transactions on Antennas and Propagation*, vol. 60, no. 7, pp. 3222–3230, July 2012.

[10] R. Long, J. Ouyang, F. Yang, W. Han, and L. Zhou, "Fast Amplitude-Only Measurement Method for Phased Array Calibration," *IEEE Transactions on Antennas and Propagation*, vol. 65, no. 4, pp. 1815–1822, April 2017.